Sampled-data observer design for sensorless control of wind energy conversion system with PMSG

Mohammed Hicham Zaggaf, Adil Mansouri, Abdelmounime El Magri, Aziz Watil, Rachid Lajouad, Lhoussain Bahatti

EEIS Laboratory, ENSET Mohammedia, Hassan II University of Casablanca, Mohammedia, Morocco

Article Info	ABSTRACT
	This paper presents a nonlinear observer for a variable-speed wind energy conversion system (WECS) utilizing a permanent magnet synchronous generator (PMSG). The study addresses the design of high-gain sampled-data observers based on the nonlinear WECS model, supported by formal convergence analysis. An essential aspect of this observer design is the incorporation of a time-varying gain, significantly enhancing system performance. Convergence of estimation errors is demonstrated using the input-to-state stability method. Simulation of the proposed observer is conducted using the MATLAB-Simulink tool. The obtained results are presented and analyzed to showcase the overall effectiveness of the proposed system.

Corresponding Author:

Mohammed Hicham Zaggaf
EEIS Laboratory, ENSET Mohammedia, Hassan II University of Casablanca
Mohammedia, Morocco
Email: h.zaggaf@gmail.com

1. INTRODUCTION

Compared to the other aero-generator, permanent magnet synchronous generators (PMSGs) enjoy better mass-power ratio and better efficiency. These features are a consequence of the fact that PMSGs Joule losses are substantially less significant because such machines have no rotor currents and no damper windings. Additionally, PMSGs find application in variable speed wind turbines, enabling direct coupling to the turbine without the use of a gearbox. This design choice avoids potential drawbacks such as reduced system availability and increased weight [1], [2]. To this end, wind energy con-version system (WECS) have now been made controlable through converters. The latter enable control over stator phases and injected currents into the grid. The action on the switches depends on the position of the electric rotor and grid frequency. Thus, the PMSGs operate at variable speeds across time.

The controllers of inverters need online measurements of the load torque, rotor speed, grid frequency and voltage grid [3]-[5]. Implementing control strategies is often facilitated by installing sensors on both the grid side and rotor side. However, this approach tends to raise system costs, compromise control system reliability.

Additionally, it may not always be feasible to deploy sensors for every state variable. Signal injection techniques were suggested using phase inductance variation to inject highfrequency signals. This method offers rotor location data when operating stationary and at moderate speeds [6], [7].

However, it requires some saliency in the machine. Injecting high frequency signals is not recommended for high-speed operations. Bolognani *et al.* [8], fundamental excitation techniques based on the identification of rotor position from stator voltages have been presented. The researchers [9]-[12], Kalman filters are invoked to estimate the induced voltage that used to determine the rotor position. This method performs well in high and medium-speed, but it is inaccurate in low-speed operations with a low back EMF. Bernard *et al.* [13], a Kalman-like linked observer was proposed. On the other hand, their study of convergence relies on an excitation condition that incorporates information from observers, including state estimations. A common characteristic of all previous observers is their continuous-time nature i.e. they need online measurements of the system continuous-time output signals. As a matter of fact, in most practical applications, system outputs are only available at sampling instants. As long as linear systems are considered, this is not an issue because exact representation of continuous-time models with discrete-time models is possible.

Therefore, there has been significant attention devoted to the development of sampled-data observers for continuous-time nonlinear systems. One effective strategy is to employ approximate discrete-time models generated through techniques akin to Euler discretization. These observers, utilizing these manageable discrete-time models, give state estimations at sampling intervals and are typically proven to ensure semi-global practical stability of the error-observation, as evidenced in works such as [14], [15]. Discrete-continuous time observers entail splitting the observation process into prediction and correction tasks, carried out between successive sampling times and solely at sampling times, respectively. This sampled-data observer proves advantageous in expanding the range of sampling period values while preserving global exponential convergence of the observer [16].

In the present study, we seek the development of sampled-data WECS with PMSG observers. The ability of the observer to provide precise estimations is referred to as the sensorless characteristic of the conversion system state variables using just sampled measurements of the system's outputs. The observer design is performed on the basis of the WECS nonlinear model described in the (α, β)-coordinate. The observer design begins with a nonlinear transformation of the initial (more physical) model into a triangular canonical shape to which the high-gain approach proves to be applicable. Nonlinear transformations are guaranteed to occur and be invertible if the model is observable [17], [18]. In light of the established canonical structure, a ZOH-innovation high-gain type observer has been developed and explicitly demonstrated to be exponentially converging. Several simulations are used to demonstrate the impact of different design elements, including the sample interval, on observer performance.

2. WECS MODELLING AND MODEL TRANSFORMATION
2.1. WECS mathematical model

The WEC system, depicted in Figure 1, comprises both a synchronous aerogenerator-converter combination and a three-phase inverter. Since the rotor position, the grid voltages and the grid frequency are expected to be inaccessible for measurement, the wind energy conversion system model is expressed in the (α, β)-reference. According to [19]-[22], the WECS model is established through the subsequent in (1).
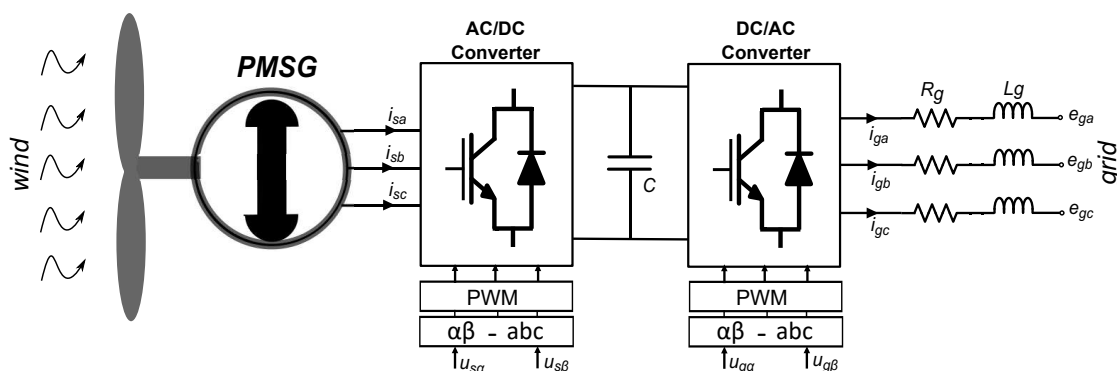

Figure 1. The WECs scheme

$$
\begin{cases}
\frac{di_{s_\alpha}}{dt} = -\frac{R_s}{L_s}i_{s_\alpha} + \frac{p\Omega}{L_s}\phi_{r_\beta} + \frac{1}{L_s}u_{s_\alpha} \\[4pt]
\frac{di_{s_\beta}}{dt} = -\frac{R_s}{L_s}i_{s_\beta} - \frac{p\Omega}{L_s}\phi_{r_\alpha} + \frac{1}{L_s}u_{s_\beta} \\[4pt]
\frac{di_{g_\alpha}}{dt} = -\frac{R_g}{L_g}i_{g_\alpha} - \frac{e_{g_\alpha}}{L_g} + \frac{u_{g_\alpha}}{L_g} \\[4pt]
\frac{di_{g_\beta}}{dt} = -\frac{R_g}{L_g}i_{g_\beta} - \frac{e_{g_\beta}}{L_g} + \frac{u_{g_\beta}}{L_g}
\end{cases}
\qquad
\begin{cases}
\frac{d\phi_{r_\alpha}}{dt} = -p\Omega\phi_{r_\beta} \\[4pt]
\frac{d\phi_{r_\beta}}{dt} = p\Omega\phi_{r_\alpha} \\[4pt]
\frac{de_{g_\alpha}}{dt} = \omega_g\sqrt{e_{g_\alpha}^2 + e_{g_\beta}^2}\cos(\theta_g) \\[4pt]
\frac{de_{g_\beta}}{dt} = \omega_g\sqrt{e_{g_\alpha}^2 + e_{g_\beta}^2}\sin(\theta_g)
\end{cases}
$$

$$
\begin{cases}
\frac{d\Omega}{dt} = -\frac{F}{J}\Omega + \frac{p}{J}(\phi_{r\alpha}i_{s\beta} - \phi_{r\beta}i_{s\alpha}) - \frac{T_g}{J} \\[4pt]
\frac{dT_g}{dt} = \delta_1(t) \\[4pt]
\frac{d\theta_g}{dt} = \omega_g \\[4pt]
\frac{d\omega_g}{dt} = \delta_2(t)
\end{cases}
\tag{1}
$$

Where L_s and R_s (resp. L_g and R_g) are the stator (resp. network) inductance and resistor; the angular rotor speed is Ω; the rotor inertia, viscosity coefficient, and number of pole pairs are denoted by the variables J, F, and p. The (α, β)-coordinates represent the following: the stator currents are $(i_{s_\alpha}, i_{s_\beta})$, rotor fluxes are $(\phi_{r_\alpha}, \phi_{r_\beta})$, and stator voltages are $(u_{s_\alpha}, u_{s_\beta})$. T_g represents the generator's load torque. The grid pulsation and electrical position are represented by ω_g and θ_g, respectively. The injected currents, grid voltages and input control are represented by $(e_{g_\alpha}, e_{g_\beta})$, $(i_{g_\alpha}, i_{g_\beta})$, and $(u_{g_\alpha}, u_{g_\beta})$.

It is necessary to observe that the mechanical torque generated through the wind's kinetic energy changes slowly over time due to the WECS's high inertia, particularly the turbine/rotor. As a result, the dynamic behavior of the generator torque, written as $\dot{T}_g = \delta_1(t)$, is defined by an undefined but bounded function. The system model is reconstructed with the following notations for clarity:

$$
x = \begin{pmatrix} x_1 \\ x_2 \\ x_3 \end{pmatrix}; \quad
u = \begin{pmatrix} u_{s\alpha} \\ u_{s\beta} \\ u_{g\alpha} \\ u_{g\beta} \end{pmatrix}; \quad
x_1 = \begin{pmatrix} x_{11} \\ x_{12} \\ x_{13} \\ x_{14} \end{pmatrix} = \begin{pmatrix} i_{s\alpha} \\ i_{s\beta} \\ i_{g\alpha} \\ i_{g\beta} \end{pmatrix};
$$
$$
x_2 = \begin{pmatrix} x_{21} \\ x_{22} \\ x_{23} \\ x_{24} \end{pmatrix} = \begin{pmatrix} \phi_{r\alpha} \\ \phi_{r\beta} \\ e_{g\alpha} \\ e_{g\beta} \end{pmatrix}; \quad
x_3 = \begin{pmatrix} x_{31} \\ x_{32} \\ x_{33} \\ x_{34} \end{pmatrix} = \begin{pmatrix} \Omega \\ T_g \\ \theta_g \\ \omega_g \end{pmatrix}
\tag{2}
$$

where the system input vector is represented by u, while the output state vector, accessible for measurement, is denoted as x_1 (corresponding to currents). The electromagnetic variables, grouped as x_2, and the mechanical and electrical network parameters, collectively labeled as x_3, are both unavailable. The symbols $\mathbb{O}_k$ and $\mathbb{I}_k$ represent the $(k \times k)$ null matrix and the $(k \times k)$ identity matrix, respectively. Additionally, the rectangular $(k \times m)$ null matrix is symbolized as $0_{(k \times m)}$.

With these notations, the mathematical model (1) may be rewritten in the following shortened shape:

$$
\begin{cases}
\dot{x} & = f(x(t), u(t)) + \delta(t) \\
y & = Cx = x_1
\end{cases}
\tag{3}
$$

with:

$$
f(x, u) \triangleq \begin{pmatrix} f_1(x, u) \\ f_2(x, u) \\ f_3(x, u) \end{pmatrix}; \quad
\delta(t) = \begin{bmatrix} \mathbb{O}_{1\times 9} & \delta_1(t) & 0 & \delta_2(t) \end{bmatrix}^T; \quad
C = \begin{bmatrix} \mathbb{I}_4 & \mathbb{O}_4 & \mathbb{O}_4 \end{bmatrix}
$$

with:

$$f_1(.) = \begin{pmatrix} -\frac{R_s}{L_s}x_{11} + \frac{p}{L_s}x_{31}x_{22} + \frac{1}{L_s}u_{s_\alpha} \\ -\frac{R_s}{L_s}x_{12} - \frac{p}{L_s}x_{31}x_{21} + \frac{1}{L_s}u_{s_\beta} \\ -\frac{R_g}{L_g}x_{13} - \frac{1}{L_g}x_{23} + \frac{1}{L_g}u_{g_\alpha} \\ -\frac{R_g}{L_g}x_{14} - \frac{1}{L_g}x_{24} + \frac{1}{L_g}u_{g_\beta} \end{pmatrix} ; f_2(.) = \begin{pmatrix} -px_{31}x_{22} \\ px_{31}x_{21} \\ x_{34}\sqrt{x_{23}^2 + x_{24}^2}\cos(x_{33}) \\ x_{34}\sqrt{x_{23}^2 + x_{24}^2}\sin(x_{33}) \end{pmatrix} ;$$

$$f_3(.) = \begin{pmatrix} -\frac{F}{J}x_{31} + \frac{p}{J}(x_{21}x_{12} - x_{22}x_{11}) - \frac{x_{32}}{J} \\ 0 \\ x_{33} \\ 0 \end{pmatrix}$$

2.2. Canonical form transformation

To utilize a high-gain observer directly, the system described by (1) needs to be transformed into a canonical form. For this transformation to be feasible, the model must be observable [23], provided such a conversion exists and is reversible. We consider the following satate transformation as consider this system (3). There is a Lipschitzian diffeomorphism $\Phi(x)$.

$$\Phi(x) : \mathbb{R}^{12} \to \mathbb{R}^{12}, x \to z = \begin{pmatrix} z_1 \\ z_2 \\ z_3 \end{pmatrix} = \Phi(x) = \begin{pmatrix} \phi_1(x) \\ \phi_2(x) \\ \phi_3(x) \end{pmatrix} \tag{4}$$

Such that the initial system representation (3) rewrites, in terms of the state vector z, in the triangular shape:

$$\begin{cases} \dot{z}(t) = Az(t) + \psi(z,u) + B\beta(z)\delta(t) \\ y(t) = z_1 = Cz(t) \end{cases} \tag{5}$$

with:

$$A = \begin{bmatrix} \mathbb{O}_4 & \mathbb{I}_4 & \mathbb{O}_4 \\ \mathbb{O}_4 & \mathbb{O}_4 & \mathbb{I}_4 \\ \mathbb{O}_4 & \mathbb{O}_4 & \mathbb{O}_4 \end{bmatrix} ; B = \begin{bmatrix} \mathbb{O}_4 \\ \mathbb{O}_4 \\ \mathbb{I}_4 \end{bmatrix} ; C = \begin{bmatrix} \mathbb{I}_4 & \mathbb{O}_4 & \mathbb{O}_4 \end{bmatrix} ;$$

$$\psi(z,u) = \begin{bmatrix} \psi_1(z_1,u) \\ \psi_2(z_1,z_2) \\ \psi_3(x,u) \end{bmatrix} ; \quad \beta(z)\delta(t) = \begin{bmatrix} -\frac{p}{JL_s}x_{22}\delta_1(t) \\ \frac{p}{JL_s}x_{21}\delta_1(t) \\ -\frac{E_g}{L_g}\cos(x_{33})\delta_2(t) \\ -\frac{E_g}{L_g}\sin(x_{33})\delta_2(t) \end{bmatrix} \tag{6}$$

$$\psi_1(z_1,u) = \begin{bmatrix} -\frac{R_s}{L_s}\mathbb{I}_2 & \mathbb{O}_2 \\ \mathbb{O}_2 & -\frac{R_g}{L_g}\mathbb{I}_2 \end{bmatrix} z_1 + \begin{bmatrix} \frac{1}{L_s} & \frac{1}{L_s} & \frac{1}{L_g} & \frac{1}{L_g} \end{bmatrix}^T u; \quad \psi_2(z_1,z_2) =$$

$$\begin{bmatrix} -\frac{F}{J}\mathbb{I}_2 & \mathbb{O}_2 \\ \mathbb{O}_2 & \mathbb{O}_2 \end{bmatrix} z_2\psi_3(x) = \frac{\partial\phi_3(x)}{\partial x_1}\dot{x}_1 + \frac{\partial\phi_3(x)}{\partial x_2}\dot{x}_2 + \frac{\partial\phi_3(x)}{\partial x_{31}}\dot{x}_{31} + \frac{\partial\phi_3(x)}{\partial x_{33}}\dot{x}_{33} \tag{7}$$

finally, the definition of the transformation $\Phi(x)$ is constructively established in the proof of the proposition.

2.3. Observability analysis

Because its triangular form, the system (5) is structurally observable, independently of the input u. It turns out that, the system (1) is observable provided that the state transformation $\Phi(x)$ exists and is regular almost everywhere [24]. In addition to that, the sufficient conditions can be written as (8).

$$E_g^2\omega_g\Omega^3\phi_r^2 \neq 0 \tag{8}$$

The PMSG rotor flux norm ($\phi_r = \sqrt{\phi_{r\alpha}^2 + \phi_{r\beta}^2}$) is a nonzero and constant. The AC-grid amplitude and frequency are also non-zero. It turns out that the transformation $\Phi(x)$ is a diffeomorphism, consequently, the system (5) is uniformly observable.

3. SAMPLED-DATA OBSERVER DESIGN

One proposes a state observer for system (1). Using only sampled measurements of the aero-generator and line grid currents $i_{s\alpha\beta}$, $i_{g\alpha\beta}$ measurements, the objective is to provide, on-line, estimations of $i_{s\alpha\beta}$, $i_{g\alpha\beta}$, $\phi_{r\alpha\beta}$, $e_{g\alpha\beta}$, Ω, T_g, θ_g and ω_g. In this regard, it is worth noting that synchronous aero-generator-DC/AC-Grid controllers are often constructed using the dq-model, this needs online measurements of many state variables, including mechanical rotor and electric grid position. The mechanical rotor position (θ_g) can be determined online using state estimates of the rotor flux ($\hat{\phi}_{r\alpha}$, $\hat{\phi}_{r\beta}$) and state estimates of the AC-grid ($\hat{e}_{g\alpha}$, $\hat{e}_{g\beta}$) using in (9):

$$\begin{aligned} \theta(t) &= \tfrac{1}{p}\theta_e(t) = \tfrac{1}{p}atan\left(\frac{\hat{\phi}_{r\beta}(t)}{\hat{\phi}_{r\alpha}(t)}\right) \\ \theta_g(t) &= atan\left(\frac{\hat{e}_{g\beta}(t)}{\hat{e}_{g\alpha}(t)}\right) \end{aligned} \tag{9}$$

where θ, θ_e and θ_g denote the mechanical, electrical PMSG position and AC-grid EMF position respectively.

3.1. Observer design and analysis in z-coordinates

The problem of designing an observer for the initial system model (3) is easier to deal with based on the equivalent model (5).

$$\begin{cases} \dot{z} = A\,z + \psi(z,u) + B\,\beta(z)\delta(t) \\ y = z_1 = C\,z \end{cases} \tag{10}$$

The technical assumptions for observer design and analysis are:

- A1: $\psi(z,u)$ is a function that is globally Lipschitz, i.e., $\exists \beta_0 > 0$, $\forall(z,\hat{z}) \in \mathbb{R}^n$: $|\psi(\hat{z},u) - \psi(z,u)| \le \beta_0|\hat{z} - z|$.
- A2: the norm of the aerogenerator rotor flux ($\phi_r = \sqrt{\phi_{r\alpha}^2 + \phi_{r\beta}^2}$) is all time nonzero and constant, (which ensures that $\beta(z)$ defined by (6) is bounded). On the other hand, $\delta(t)$ is unknown and bounded function, i.e $\exists N_1 > 0$: $\beta(z)\delta(t) < N_1$.

Inspired by [25], the following sampled-data observer is considered:

$$\begin{cases} \dot{\hat{z}} = A\hat{z} + \psi(\hat{z},u) - \Delta^{-1}\theta K\phi(t)(C\hat{z}(t_k) - y(t_k)) & t \in [t_k, t_{k+1}) \\ \dot{\phi}(t) = -\eta\phi(t)^a, & \forall t \in [t_k, t_{k+1}), \forall k \in \mathbb{N} \\ \phi(t_k) = 1, \end{cases} \tag{11}$$

with,

$$\Delta = diag\left(\mathbb{I}_4, \frac{1}{\theta}\mathbb{I}_4, \frac{1}{\theta^2}\mathbb{I}_4\right) \tag{12}$$

a and η are a scalars constants satisfying $0 < a \le 1$ and $\eta > 0$. The later are design parameters used to tune the rate of the time varying gain $\phi(t)$ which acts as a forgetting factor between any two successive sampling times. The $K \in \mathbb{R}^{12 \times 12}$-matrix gain is selected so that the matrix $(A - KC)$ is Hurwitz. This ensures that, for any scalar $\mu > 0$, there is a positive definite matrix P satisfying the following Lyapunov function:

$$(A - KC)^T P + P(A - KC) \le -\mu\mathbb{I}_{12} \tag{13}$$

As previously indicated, the function $\phi(t)$ serves as a factor for data attenuation within the intervals $[t_k, t_{k+1})$. At each discrete sampling instant, this function has been modified to its maximum value, unity, with the aim of restoring the continuous-time observer whenever a measurement becomes available. To ensure that the function $\phi(t)$ remains strictly positive, an appropriate upper bound for the maximum allowable sampling period T_{max} is selected. More specifically, the function $\phi(t)$ is designed to decrease over the time interval (t_k, t_{k+1}), thereby mitigating the impact of measurement errors.

Theorem 1: take the system (10) with Assumptions $A1$ and $A2$. Define the scalar parameters shown in (14).

$$\begin{cases} \theta_0 = sup\{1, \frac{2\beta_0}{\mu}\frac{\lambda_M}{\lambda_m}||P||\} \\ \sigma_0 = \frac{\mu(\theta - \theta_0)}{2\lambda_M}; \quad \sigma_1 = \frac{\theta||PK||}{\sqrt{\lambda_m}}; \quad \sigma_2 = \frac{N_1}{\theta^2}\frac{||P||}{\sqrt{\lambda_m}} \end{cases} \tag{14}$$

Let the maximum sampling period T_{max} be selected in accordance with the following inequality in (15).

$$T_{\max} \leq \frac{\sigma_0 \sqrt{\lambda_m}}{\sigma_1(\theta + \beta_0 + \theta|K| + \eta)} \tag{15}$$

Then, for all $\theta > \theta_0$ and all $T_s \in (0, T_{max}]$, the state estimation error $\tilde{z}$ converges, to a neighborhood of the origin that can be made arbitrarily small by letting the θ be sufficiently large, whatever the initial condition $\tilde{z}(0)$.

Remark 1: it is readily checked that the solution of the differential equation $\dot{\phi} = -\eta\phi(t)^a$ with $0 < a < 1$ converges to zero in a finite time t_f stated as (16).

$$t_f = \frac{1}{\eta(1-a)}. \tag{16}$$

More explicitly, the solution of the above differential equation $\dot{\phi}$, when the sampling period is smaller than $\frac{1}{\eta(1-a)}$, expresses as (17).

$$\begin{cases} \phi(t) = (1 - \eta(1-a)(t - t_k))^{\frac{1}{1-a}}, & \forall t \in [t_k, t_{k+1}) \\ \phi(t_k) = 1, & k \in \mathbb{N} \end{cases} \tag{17}$$

If the sampling period is more than $\frac{1}{(1-a)\eta}$, i.e., $T_s > t_f$, the changing gain $\phi(t)$ will be equal to zero between $[t_k + t_f, t_{k+1})$, and the observer will simply be a copy of the system (3). This means that, throughout time intervals $[t_k + t_f, t_{k+1})$, the effect of measurement errors in the observation error will be ignored.

3.2. Observer in x-coordinates

In the preceding subsection, for the system given by (1) in z-coordinates, we constructed a state observer. To make implementation easier, the specified observer should be translated into the original x-coordinates. The theorem that follows focuses on this transition.

Theorem 2: considering the system (3) under Assumptions $A1$ and $A2$. Let the scalar parameters (θ_0, σ_0) be chosen as in (14) and the maximum sampling period T_{max} be selected in accordance with the inequality (15). Then, for all $\theta > \theta_0$ and all $T_s \in (0, T_{max}]$, one has:

- The systems (2.1.) are observed by the following system:

$$\begin{cases} \dot{\hat{x}} = f(\hat{x}, u) - \Lambda^{-1}\theta\Delta^{-1}K\phi(t)(C\hat{z}(t_k) - y(t_k)) & t \in [t_k, t_{k+1}) \\ \dot{\phi}(t) = -\eta\phi(t)^a, & \forall t \in [t_k, t_{k+1}), \forall k \in \mathbb{N} \\ \phi(t_k) = 1, \end{cases} \tag{18}$$

  with $\Lambda = \frac{d\Phi}{dx}$ denote the Jacobian of $\Phi(x)$ and Δ, C are respectively given by (12) and (6) and gain $K \in \mathbb{R}^{12 \times 12}$.

- The state estimation error $\tilde{x} = \hat{x} - x$ converges to a neighborhood at the origin that may be made arbitrarily tiny by allowing the θ to be sufficiently big, regardless of the initial condition $\tilde{x}(0)$.

Proof:

- The derivative of the estimate $\hat{z} = \Phi(\hat{x})$ may be written as $\dot{\hat{z}} = \Lambda\dot{\hat{x}}$, resulting in the following:

$$\dot{\hat{x}} = \Lambda^{-1}(\hat{x})\dot{\hat{z}} \tag{19}$$

  On the other hand, using (3), (4), and (10) one can see that : $A\hat{z} + \psi(\hat{z}, u) = \Lambda f(x, u)$. According to (11), the dynamical system (18) observes the system expressed through its model (3).

- The Jacobian Λ of the state transformation Φ has complete rank practically everywhere. Since $\Phi(x)$ is a difeomorphism, any $(x, \hat{x}) \in \mathbb{R}^{12 \times 2}$ corresponds to a unique $(z, \hat{z}) \in \mathbb{R}^{12 \times 2}$, and vice versa. According to the Theorem 1, for all $\theta > \theta_0$ and all $T_s \in (0, T_{max}]$, the state estimation error $\tilde{z} = \hat{z} - z = (\Phi(\hat{x}) - \Phi(x))$ converge, to a neighborhood of the origin that can be made arbitrarily small by letting the θ be sufficiently large, whatever the initial condition $\tilde{z}(0) = (\Phi(\hat{x}(0)) - \Phi(x(0)))$.

4. SIMULATION RESULTS

The proposed observer's performance will be assessed through numerical simulations. The system depicted in Figure 1 is simulated, with power electronics components modeled using the SimPower toolbox. This system comprises a PMSG linked to the AC grid via power converters. The parameters specified in Table 1 correspond to a system power of approximately $3 kW$. Implementing the sampled-data high-gain observer (SDHGO) (18) is achieved using Matlab/Simulink resources, particularly the control system toolbox. The control's effectiveness hinges on the numerical values assigned to the observer parameters θ, η, K, a, and the sampling period T_s. Following iterative adjustments, the numerical values listed in Table 2 have been selected as appropriate.

Table 1. WECs characteristics

Characteristic	Symbol and value	Characteristic	Symbol and value
Wind turbine		Total inertia	$J = 0.1\, Nm/rd/s^2$
Nominal power	$P_t = 3kW$	Total viscous friction	$f = 0.07\, Kg.m^2.s^{-1}$
Turbine radius	$R = 1.3\, m$	AC-DC-AC converter	
Blade pitch	$\beta = 2°$	Capacitor	$C = 47\, mF$
Aero-generator		Inductor	$L_g = 0.05\, H$
Nominal power	$P_n = 3.00kW$	Resistor	$R_g = 0.5\, \Omega$
Number of pole pairs	$p = 5$	DC-Link voltage	$V_{dc} = 700\, V$
Nominal speed	$\Omega_n = 60\, rd/s$	Modulation frequency	$F_m = 15\, kHz$
Stator resistor	$R_s = 0.6\Omega$	Three-phase network	
Stator cyclic inductor	$L_s = 0.0094\, H$	Voltage	$E_g = 230/400\, V$
Rotor flux	$\phi_r = 0.3\, Wb$	Network frequency	$f_g = 50\, Hz$

Table 2. Observer parameters numerical values

Parameter	θ	K	η	a	T_s
Value	180	$[5\,\mathbb{I}_4\ 10\,\mathbb{I}_4\ 5\,\mathbb{I}_4]^T$	500	0.5	$1.5\, ms$

The observer's performance (18) will be assessed in the context of fluctuating wind speed over time. The observer's design does not explicitly account for changes in the external generator torque or grid settings. That is, the observer compensates for their influence, which is comparable to the beginning conditions reset, due to its global convergence nature. The observer convergence allows for any beginning values ($\hat{\phi}(0)$, $\hat{\Omega}(0)$, and $\hat{T}_g(0)$). The sensitivity of the observer performances to the sampling period value will be illustrated. To this end, the sampling period is successively given the values: $T_s = 2.5\, ms$ (with $\eta = 500$, $a = 1$), $T_s = 2.8\, ms$ (with $\eta = 500$, $a = 0.5$), and $T_s = 3\, ms$ (with $\eta = 500$, $a = 0.25$).

Clearly, the observer is performing well. Despite the substantial initial estimation error, the observer's estimations rapidly converge to unknown values. Figure 2 shows the rotor speed and its estimated value. The observer's speed estimate (18) closely matches the real speed, and both signals align with the reference trajectory. Figures 3-4 show that the rotor position, generator torque, $\alpha\beta$-components ($\phi_{r\alpha}$; $\phi_{r\beta}$) of PMSG rotor flux (Figure 5), $\alpha\beta$-components ($e_{g\alpha}$; $e_{g\beta}$) (Figure 6) of grid voltage and frequency (ω_g) (Figure 7) perfectly converge to their true values. Finally, it is checked that the time-varying gain observer (18) allows larger sampling periods compared to the constant gain observer obtained by letting $\phi(t) = 1$ in (18). The comparison is made considering different values of the design parameter a of the time-varying gain observer (18). Figures 2-7 see in (APPENDIX).

5. CONCLUSION

The focus of this study is on the online estimation of critical parameters such as rotor position, turbine speed, load torque, grid voltage, and frequency in wind energy conversion systems. While existing state observers theoretically address this challenge, they are hindered by limitations such as the requirement for continuous-time measurements of system outputs and the need for persistently exciting signals. These constraints render previously proposed observers less suitable for practical applications. In this work, a novel observer is introduced to overcome these limitations. Notably, this observer operates in a sampled-data framework, eliminating the necessity for continuous-time measurements and persistently exciting input signals. This achievement is realized through a combination of the high-gain design approach and the zero-order hold (ZOH)-innovation principle. An additional innovation in this study is the incorporation of a resetting adaptation gain at sampling times. This resetting feature has proven advantageous in expanding the range of admissible sampling periods.
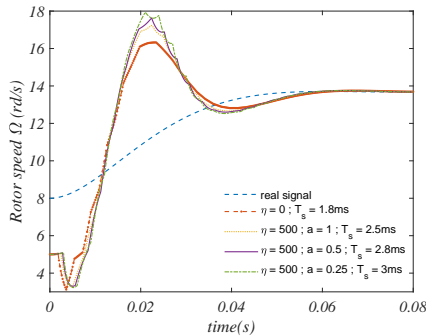
APPENDIX

Figure 2. Rotor speed variation: true speed and its estimates with different values of the design parameters
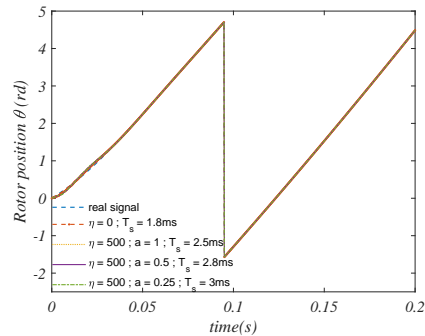

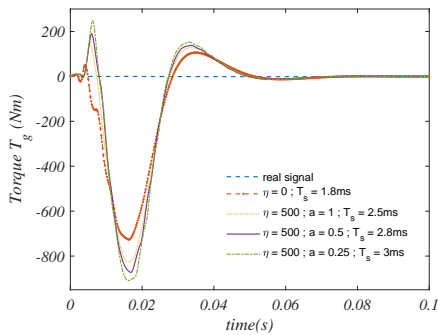Figure 3. Rotor position: true position and its estimates with different values of the design parameters

Figure 4. Generator torque variation: true torque and its estimate with different values of the design parameters
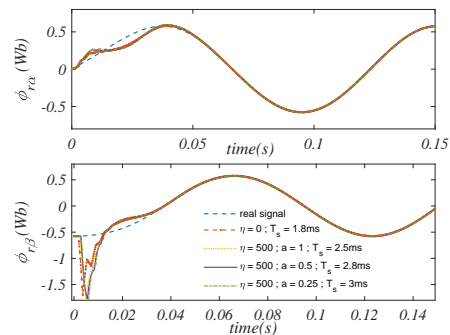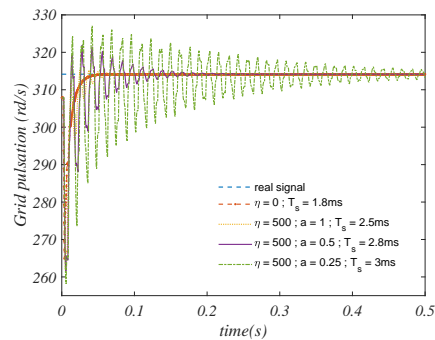

Figure 5. Rotor flux variation: true flux and its estimates with different values of the design parameters. Top. α-axis flux, Bottom. β-axis flux
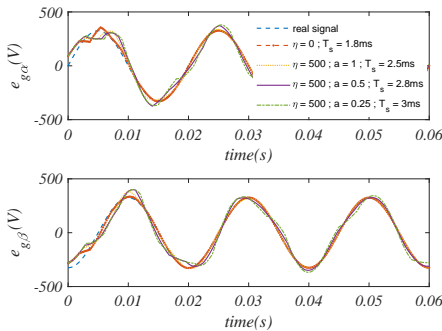
Figure 6. Grid voltage: true voltage and its estimates with different values of the design parameters. Top. α-axis voltage, Bottom β-axis voltage

Figure 7. Grid frequency variation: true frequency and its estimates with different values of the design parameters

REFERENCES

[1]   C. Chatri, M. Labbadi, and M. Ouassaid, "Improved high-order integral fast terminal sliding mode-based disturbance-observer for the tracking problem of PMSG in WECS," *International Journal of Electrical Power and Energy Systems (IJEPES0*, vol. 144, p. 108514, Jan. 2023, doi: 10.1016/j.ijepes.2022.108514.
[2]   A. El Magri, F. Giri, G. Besançon, A. El Fadili, L. Dugard, and F. Z. Chaoui, "Sensorless adaptive output feedback control of wind energy systems with PMS generators," *Control Engineering Practice*, vol. 21, no. 4, pp. 530–543, Apr. 2013, doi: 10.1016/j.conengprac.2012.11.005.

[3]   J. Chen, W. Yao, C. K. Zhang, Y. Ren, and L. Jiang, "Design of robust MPPT controller for grid-connected PMSG-Based wind turbine via perturbation observation based nonlinear adaptive control," *Renewable Energy*, vol. 134, pp. 478–495, Apr. 2019, doi: 10.1016/j.renene.2018.11.048.

[4]   N. Elaadouli, R. Lajouad, A. El Magri, A. Watil, A. Mansouri, and I. El Myasse, "An improved control for a stand-alone WEC system involving a Vienna rectifier with battery energy storage management," *Journal of Energy Storage*, vol. 76, p. 109716, Jan. 2024, doi: 10.1016/j.est.2023.109716.

[5]   A. Mansouri, A. El Magri, I. El Myasse, R. Lajouad, and N. Elaadouli, "Backstepping nonlinear control of a five-phase PMSG aerogenerator linked to a Vienna rectifier," *Indonesian Journal of Electrical Engineering and Computer Science (IJEECS)*, vol. 32, no. 2, p. 734, Nov. 2023, doi: 10.11591/ijeecs.v32.i2.pp734-741.

[6]   H. Zatocil, "Sensorless control of AC machines using high-frequency excitation," in *2008 13th International Power Electronics and Motion Control Conference*, EPE-PEMC 2008, Sep. 2008, pp. 1024–1032, doi: 10.1109/EPEPEMC.2008.4635402.

[7]   S. Ichikawa, M. Tomita, S. Doki, and S. Okuma, "Sensorless control of permanent-magnet synchronous motors using online parameter identification based on system identification theory," *IEEE Transactions on Industrial Electronics*, vol. 53, no. 2, pp. 363–372, Apr. 2006, doi: 10.1109/TIE.2006.870875.

[8]   S. Bolognani, L. Tubiana, and M. Zigliotto, "Extended Kalman filter tuning in sensorless PMSM drives," *IEEE Transactions on Industry Applications*, vol. 39, no. 6, pp. 1741–1747, Nov. 2003, doi: 10.1109/TIA.2003.818991.

[9]   M. Huang, Z. Wei, J. Zhao, R. A. Jabr, M. Pau, and G. Sun, "Robust ensemble kalman filter for medium-voltage distribution system state estimation," *IEEE Transactions on Instrumentation and Measurement*, vol. 69, no. 7, pp. 4114–4124, Jul. 2020, doi: 10.1109/TIM.2019.2945743.

[10]   A. Kashaganova, K. Suleimenov, S. Sagnaeva, and T. D. Do, "Maximum power tracking for wind energy conversion systems via a high-order optimal disturbance observer-based LQR without a wind speed sensor," *Engineering Science and Technology, an International Journal*, vol. 45, p. 101472, Sep. 2023, doi: 10.1016/j.jestch.2023.101472.

[11]   B. Lang, W. Liu, and G. Luo, "A new observer of stator flux linkage for permanent magnet synchronous motor based on Kalman Filter," *ICIEA 2007: 2007 Second IEEE Conference on Industrial Electronics and Applications*, pp. 1813–1817, 2007, doi: 10.1109/ICIEA.2007.4318723.

[12]   Z. Wang, Y. Zheng, Z. Zou, and M. Cheng, "Position sensorless control of interleaved CSI fed PMSM drive with extended Kalman filter," *IEEE Transactions on Magnetics*, vol. 48, no. 11, pp. 3688–3691, Nov. 2012, doi: 10.1109/TMAG.2012.2197180.

[13]   P. Bernard, N. Mimmo, and L. Marconi, "On the semi-global stability of an ek-like filter," *IEEE Control Systems Letters*, vol. 5, no. 5, pp. 1771–1776, Nov. 2021, doi: 10.1109/LCSYS.2020.3044030.

[14]   A. El Assoudi, E. H. El Yaagoubi, and H. Hammouri, "Non-linear observer based on the Euler discretization," *International Journal of Control*, vol. 75, no. 11, pp. 784–791, Jan. 2002, doi: 10.1080/00207170210141860.

[15]   D. Zhang, Y. Shen, J. Mei, and Z.-H. Guan, "Sampled-data observer design for a class of nonlinear systems with applications," in *17th International Symposium on Mathematical Theory of Networks and Systems*, 2006, pp. 3–7.

[16]   H. Hammouri, P. Kabore, S. Othman, and J. Biston, "Failure diagnosis and nonlinear observer. Application to a hydraulic process," *Journal of the Franklin Institute*, vol. 339, no. 4–5, pp. 455–478, Jul. 2002, doi: 10.1016/S0016-0032(02)00027-3.

[17]   J.-P. Gauthier and I. Kupka, *Deterministic Observation Theory and Applications*. Cambridge University Press, 2001.

[18]   M. Farza, M. M'Saad, and L. Rossignol, "Observer design for a class of MIMO nonlinear systems," *Automatica*, vol. 40, no. 1, pp. 135–143, Jan. 2004, doi: 10.1016/j.automatica.2003.08.008.

[19]   M. H. Rashid, *Power Electronics Handbook*, 3rd ed, Academic Press, 2011.

[20]   A. El Magri, F. Giri, and A. El Fadili, "Control models for synchronous machines," in *AC Electric Motors Control: Advanced Design Techniques and Applications*, Wiley, 2013, pp. 41–56.

[21]   A. Mansouri, A. El Magri, R. Lajouad, F. Giri, M. said Adouairi, and B. Bossoufi, "Nonlinear observer with reduced sensors for WECS involving Vienna rectifiers — Theoretical design and experimental evaluation," *Electric Power Systems Research*, vol. 225, p. 109847, Dec. 2023, doi: 10.1016/j.epsr.2023.109847.

[22]   A. Ali et al., "High gain differentiator based neuro-adaptive arbitrary order sliding mode control design for MPE of standalone wind power system," *PLoS ONE*, vol. 19, no. 1 January, p. e0293878, Jan. 2024, doi: 10.1371/journal.pone.0293878.

[23]   S. Ting Goh, S. A. (Reza) Zekavat, and O. Abdelkhalik, "An introduction to Kalman filtering implementation for localization and tracking applications," in *Handbook of Position Location*, Wiley, 2018, pp. 143–195.

[24]   R. Hermann and A. J. Krener, "Nonlinear controllability and observability," *IEEE Transactions on Automatic Control*, vol. 22, no. 5, pp. 728–740, Oct. 1977, doi: 10.1109/TAC.1977.1101601.

[25]   T. Ahmed-Ali, L. Burlion, F. Lamnabhi-Lagarrigue, and C. Hann, "A sampled-data observer with time-varying gain for a class of nonlinear systems with sampled-measurements," in *Proceedings of the IEEE Conference on Decision and Control*, Dec. 2014, vol. 2015-February, no. February, pp. 316–321, doi: 10.1109/CDC.2014.7039400.

BIOGRAPHIES OF AUTHORS

Mohammed Hicham Zaggaf ⬤ 🔗 🔬 ↻ Received the Ph.D. degree in control engineering from the Université Hassan II, Casablanca, Morocco, in 2019. Currently, he is an Assistant Professor at the Ecole Normale Supérieure d'Enseignement Technique (ENSET), Hassan II University, Mohammedia, Morocco. His research interests include optimization and nonlinear control of AC machines and energy systems. He can be contacted at email: h.zaggaf@gmail.com.

Adil Mansouri Received the Aggregation of Electrical Engineering from the Normal School of Technical Education (ENSET), Rabat, Morocco, in 2013, the Ph.D. degree in Electrical engineering and Automatic from Hassan II University of Casablanca, Morocco, in 2023. Currently an Electrical Engineering professor in preparatory Engineering classes. His research interests include optimization, observation and nonlinear control of AC machines and renewable energy. He can be contacted at email: mansouri_adil@yahoo.com

Abdelmounime El Magri Received the Aggregation of Electrical Engineering from the Normal School of Technical Education (ENSET), Rabat, Morocco, in 2001, the Ph.D. degree in Electrical and control engineering from University Mohammed V, Rabat; in 2011. Currently, he is Professor at the Normal School of Technical Education, Mohammedia, University Hassan II, Casablanca, Morocco. His research interests include nonlinear system identification, nonlinear control, adaptive control, power and energy systems control. He has coauthored several papers on these topics. He can be contacted at email: magri_mounaim@yahoo.fr.

Aziz Watil He received his Ph.D. in Electrical Engineering and Automatic from Hassan II University of Casablanca, Morocco, in 2022. His research interests are focused on the study of dynamical systems, optimization, nonlinear control, and observer design for many applications including electric power systems and renewable energy conversion systems. He can be contacted at email: azizwatil@gmail.com.

Rachid Lajouad Received the Aggregation of Electrical Engineering from ENSET, Rabat, Morocco, in 2000. Earned the Ph.D. degree in control engineering from the Université Mohammed V, Rabat, Morocco, in 2016, under the supervision of Prof. F. Giri and Prof. F.Z. Chaoui. Currently, he is a Professor at the Ecole Normale Supérieure d'Enseignement Technique (ENSET), Hassan II University, Mohammedia, Morocco. His research interests include optimization, observation, and nonlinear control of AC machines and energy systems. He has co-authored several papers on these topics. He can be contacted at email: rlajouad@gmail.com.

Lhoussain Bahatti Was born in 1969 at MIDELT, Morocco. He is now a teacher of electrical engineering and researcher at Hassan II University of Casablanca, ENSET Institute, Mohammedia Morocco. He received the Aggregation Electrical Engineering degree in 1995 from the ENS CACHAN France. He has his Ph.D. degree in 2013 in musical signal processing from the Faculty of Science and Technology of Mohammedia (FSTM). He has published more than 30 research publications in various National, International conference proceedings and Journals on signal processing, control and machine learning. He is a supervisor and Co-supervisor of several PhD students in the field of identification, biomedical signal processing, smart control of renewable energy production systems and pattern recognition. He can be contacted at email: bahatti.enset@gmail.com.